Title

Light-Element Synthesis in High-Entropy Relativistic Flows Associated with Gamma-Ray Bursts

Journal

The Astrophysical Journal, 580(1)

ISSN

0004-637X

Authors

Pruet, Jason
Guiles, Shannon
Fuller, George M

Publication Date

2002-11-20

DOI

10.1086/342838

Peer reviewed

The Astrophysical Journal, 580:368–373, 2002 November 20

LIGHT-ELEMENT SYNTHESIS IN HIGH-ENTROPY RELATIVISTIC FLOWS ASSOCIATED WITH GAMMA-RAY BURSTS

Jason Pruet
Lawrence Livermore National Laboratory, 7000 East Avenue, University of California, L-414, P.O. Box 808, Livermore, CA 94551

and

Shannon Guiles and George M. Fuller
Department of Physics, 9500 Gilman Drive, University of California at San Diego, La Jolla, CA 92093-0319
Received 2002 April 23; accepted 2002 July 12

ABSTRACT

We calculate and discuss the light-element freezeout and nonthermal reaction nucleosynthesis in high-entropy winds and fireballs for broad ranges of entropy per baryon, dynamic timescales characterizing relativistic expansion, and neutron-to-proton ratios. With conditions characteristic of gamma-ray bursts (GRBs), we find that deuterium production can be prodigious, with final abundance values $^2\mathrm{H}/\mathrm{H} \gtrsim 2\%$, depending on the fireball isospin, late-time dynamics, and the effects of neutron-decoupling–induced high-energy nonthermal nuclear reactions. This implies that there could potentially be detectable local enhancements in the deuterium abundance associated with GRB events.

Subject headings: gamma rays: bursts — nuclear reactions, nucleosynthesis, abundances — stars: neutron

1. INTRODUCTION

In this paper we show that the high-entropy relativistic flows thought to accompany catastrophic stellar endpoint events such as binary neutron star mergers (Eichler et al. 1989) and collapsars (MacFadyen & Woosley 1999) may be a source of interesting light-element synthesis. In particular, we find that under the right circumstances, a significant fraction of the relativistic ejecta can be turned into ^{2}H. Although this cannot be a cosmologically significant ^{2}H source on account of the small mass and presumed low event rates associated with, e.g., GRBs, it could represent an appreciable *local* enhancement. Because the collisionless shocking (and subsequent synchrotron emission) of ultrarelativistic winds is thought to give rise to observed GRBs, deuterium production in these winds raises the possibility of a nucleosynthetic signature of the GRB environment.

The general nucleosynthesis associated with rapid adiabatic expansion and freezeout from nuclear statistical equilibrium (NSE) at high entropy per baryon s was first considered in the landmark paper by Wagoner, Fowler, & Hoyle (1967, hereafter WFH67). Those authors concentrated on the environments associated with exploding supermassive objects, where $s/k_{\mathrm{B}} \sim 10^3$, and on big bang nucleosynthesis (BBN), where $s/k_{\mathrm{B}} \approx 10^{10}$. In both supermassive objects and BBN, the conditions are expected to be proton-rich (preponderance of protons over neutrons), and the characteristic expansion timescale large (e.g., $\tau_{\mathrm{dyn}} \sim 100$ s for BBN). The physics of relativistic outflows and potential nucleosynthesis in these sites has also been the subject of some recent attention (Pruet, Fuller, & Cardall 2001; Thompson, Burrows, & Meyer 2001; Otsuki et al. 2000).

Here we extend the WFH67 study. We consider freezeout from NSE over a wide range of entropy per baryon spanning that in WFH67 and a range of neutron-to-proton ratios, all the way from proton-rich to neutron-rich. NSE freezeout in these scenarios is calculated for expansion timescales ranging from those appropriate for relativistic flows from compact objects to those associated with BBN (10^{-6} s $< \tau_{\mathrm{dyn}} < 100$ s).

We find that some general nuclear physics features of BBN are a recurring theme throughout all of these parameter ranges. In particular, ^{2}H synthesis can be significant for relativistic flows. The expected possibly neutron-rich conditions of a GRB fireball are, in a sense, the isospin mirror of those for BBN. However, we also show that it is not sufficient to simply consider only the NSE freezeout nucleosynthesis in some parameter regimes appropriate for, e.g., GRB fireballs. In fact, the dynamics of these fireballs can differ dramatically on a microscopic scale from the conditions treated by WFH67.

In particular, for initially neutron-rich material, the few protons accelerate with the relativistic photon and $e^{\pm}$ pair fluid to a very high Lorentz factor ($\gamma \sim 10^2$–10^3). In this scenario, there are high-energy ($\sim$GeV) collisions of protons on "left-behind" neutron stragglers (Fuller, Pruet, & Abazajian 2000). It has been shown that high-energy collisions of this kind can result in significant destruction and/or production of light nuclei (Dimopoulos et al. 1988). We show below that these nonthermal nuclear reactions can significantly modify the simple BBN-like NSE freezeout abundances of ^{2}H and other species. In the right conditions, ^{2}H number fraction yields can approach $Y_{\mathrm{D}} \sim 10\%$. This is a staggeringly high yield given the known, and small, primordial ^{2}H abundance.

The deuteron is a particularly interesting nucleus because it has a binding energy of only $\approx$2.2 MeV and is notoriously fragile and difficult to synthesize. At present, it is thought that essentially all of the deuterium in the universe is primordial. Estimates of the primordial $^2\mathrm{H}/\mathrm{H}$ come from measurements of the 82 km s^{-1} isotope shift in the Lyα line in a handful of high-redshift Lyman limit clouds. These are clouds that intersect our lines of sight to distant quasars (QSOs). The values of $^2\mathrm{H}/\mathrm{H}$ inferred from these clouds are consistent with each other and average to $^2\mathrm{H}/\mathrm{H} \sim 3 \times 10^{-5}$ (O'Meara et al. 2001). Because the deuterium yield in the

big bang is a sensitive function of the entropy per baryon (or alternatively, the baryon-to-photon ratio η), the observed ^{2}H/H ratio places important constraints on conditions during the epoch of BBN and gives a determination of the baryon rest mass contribution to closure (scaled by the Hubble parameter in units of 100 km s^{-1} Mpc^{-1}), $\Omega_b h^2 \approx 0.02$.

Estimates of the present-day interstellar medium (ISM) values of ^{2}H/H in different directions from the UV Lyα transition are also consistent with each other and average to about $^2\mathrm{H/H} \approx 1.5 \times 10^{-5}$ (McCullough 1992), in accord with the idea that stellar processing results in a net destruction of deuterium. There have also been a number of careful radio searches for the hyperfine transition in deuterium. So far, these have only yielded upper bounds about a factor of 4 higher than the abundance measured by UV satellites. Nonetheless, radio searches for pockets of ^{2}H in supernova remnants may represent a promising avenue for detecting evidence of relativistic flows. Ultimately, whether or not deuterium from relativistic flows is detectable depends on the interaction of the flow with the ISM. We do not calculate this here.

2. NUCLEOSYNTHESIS IN RELATIVISTIC FLOWS

The evolution of a hot plasma is governed by the initial radius R_0 of the plasma, the initial temperature of the plasma T_0, and the entropy per baryon s/k_{B} in units of Boltzmann's constant. Initially, the plasma accelerates under the influence of thermal pressure. For optically thick flows, the acceleration ceases when the thermal energy of the fireball is converted to kinetic energy. Energy conservation gives the final Lorentz factor γ_f of the fireball as

$$\gamma_f \approx \frac{E_0}{M} \ . \tag{1}$$

Here E_0 is the total initial energy (thermal plus rest mass) in the fireball and M is the mass of the baryons confined to the fireball (in this and in what follows, we set $\hbar = c = 1$). Implicit in equation (1) is the assumption that the energy density in the fireball is thermal. A portion of the energy density may be electromagnetic (Mészáros & Rees 1997; Mészáros, Laguna, & Rees 1993; Vlahakis & Königl 2001). This will alter the relation in equation (1) (and also the expression for the entropy in the flow) as well as change the nucleosynthesis.

In this paper we focus on the case in which the initial plasma is baryon poor, so $\gamma_f > 10$. Nonrelativistic or mildly relativistic outflows with modest entropy per baryon ($s/k_{\mathrm{B}} \sim 100$) can give rise to interesting heavy-element synthesis (Meyer et al. 1992; Woosley et al. 1994; Takahashi, Witti, & Janka 1994) but are relatively uninteresting as far as $A < 8$ nuclei are concerned. In terms of γ_f and the initial temperature, the entropy per baryon in the fireball is

$$\frac{s}{k_{\mathrm{B}}} \approx \gamma_f \frac{60}{45}\frac{m_p}{T_0} \approx 1250\gamma_f \left(\frac{1\ \mathrm{MeV}}{T_0}\right) \approx 10^4\text{–}10^6 \ . \tag{2}$$

Here m_p is the proton rest mass. At these entropies and for $T_0 \gtrsim 0.2$ MeV, nuclear statistical equilibrium determines that initially the fireball consists of free neutrons and protons. The neutron-to-proton ratio in these relativistic ejecta remains an open and important question because it may be a probe of conditions near the fireball source and so help pin down the physics of the central engine. When weak processes are rapid compared to the expansion timescale, n/p will come to equilibrium with these processes at $n/p \sim 1$ for T more than a few MeV. The rate of electron capture on free protons (and of positron capture on free neutrons) is $\sim (T/1\ \mathrm{MeV})^5\ \mathrm{s}^{-1}$. This means that $e^{\pm}$ capture will influence n/p if $(T/1\ \mathrm{MeV})^5 > 10^4 (10^6\ \mathrm{cm}/R_0)$. (Below we identify R_0 with the dynamic timescale.) This result implies that weak processes may or may not influence n/p depending on the details of the fireball source. For relativistic winds from neutron star–neutron star (NS-NS) mergers, for example, neutrino (and $e^{\pm}$) processes are too slow to influence n/p, so the composition of the outflow mirrors the composition of the material ablated/ejected from the neutron stars (Pruet et al. 2001). Rough estimates of n/p from different stellar and compact object sources range from $n/p \approx 10$ for NS-NS mergers to $n/p \sim 0$–1 for flows from supermassive object collapse. At any rate, this is one of the few environments in which free neutrons may be present. We treat n/p as an unknown free parameter in this work.

The acceleration of the initially hot plasma has been investigated by a number of authors. To a good approximation, the Lorentz factor and temperature in the plasma evolve simply as $\gamma = R/R_0 = T_0/T$ during the acceleration stage of the fireball's evolution and as $\gamma = \gamma_f$ for $R > R_0\gamma_f$ (Paczyński 1990). These scaling relations imply that an observer comoving with the fireball sees the temperature evolve as $T = T_0 \exp(-t/R_0)$. This determines the dynamic timescale as $\tau_{\mathrm{dyn}} = R_0$. Compact objects typically have radii of the order of 10^6 cm, implying $\tau_{\mathrm{dyn}} \sim 10^{-5}$ s. The dynamic timescale for flows from jets breaking out of massive stars during stellar collapse may be a few orders of magnitude larger (MacFadyen & Woosley 1999). Piran (1999) has argued that the dynamic timescale (τ_{dyn}) and the timescale characterizing the observed variability in the GRB (τ_{var}) are roughly equal for a broad class of central engine models. If this relation is generically true, then τ_{dyn} can be at most a few milliseconds. However, S. Woosley (2002, private communication) argues that for the collapsar model, τ_{var} can be much shorter than τ_{dyn}. The reason is that the two timescales are set by different mechanisms. The variability timescale is set by the timescale of instabilities between the outgoing jet and the stellar envelope, while the dynamic timescale is set by the surface of last interaction of the jet, which is of the order of 10^{11} cm, or a few seconds. It would be very interesting if it could be shown that the dynamic timescale and timescale of variability are always equal, because this would imply that there is far less interaction between the outgoing jet and the stellar envelope than is currently thought (if collapsars give rise to GRBs). At present it appears that the jet evolution in these collapsars is too complicated to allow reliable statements about nucleosynthesis. The validity of a simple picture for the jet evolution and associated nucleosynthesis depends on the extent of the interaction between the outgoing jet and the stellar envelope.

As the relativistic flow expands and cools, NSE begins to favor bound nuclei. As long as the reactions responsible for keeping nuclei in NSE are fast compared to the expansion timescale, the nuclear abundances will track statistical equilibrium abundances. Once the reaction rates become slow compared to τ_{dyn}, the material freezes out of NSE and breaks into successively smaller clusters of nuclei in quasi-statistical equilibrium (QSE). Below we calculate freezeout

nucleosynthesis yields in relativistic fireballs using the code developed by Kawano for BBN (Kawano 1992). First, however, we illustrate some of the salient aspects of nucleosynthesis in these relativistic fireballs by using a simplified toy reaction network.

Suppose for a moment that deuterium were the only possible bound nuclear species (i.e., flow to heavier nuclei is prevented). In this case, the evolution of the deuterium number fraction $Y_{\rm D}$ ($Y_{\rm X}$ is defined as the number density of nucleus X divided by the number density of baryons) is given by

$$\frac{dY_{\rm D}}{dt} = \rho_b Y_p Y_n \langle\sigma v\rangle_{pn{\rm D}\gamma} - Y_\gamma Y_{\rm D} \lambda_\gamma \approx \langle\sigma v\rangle_{pn{\rm D}\gamma}\left[\rho_b Y_p Y_n - 5\times 10^9 T_9^{3/2}\exp\left(-\frac{Q}{T_9}\right) Y_{\rm D}\right] . \quad (3)$$

Here $\langle\sigma v\rangle_{pn{\rm D}\gamma} \approx 4.7\times 10^4$ cm^3/(s mol) corresponds to $n(p, \gamma)$D, T_9 is the temperature in units of 10^9 K, and $Q \approx 2.2$ MeV is the binding energy of the deuteron. To a first approximation, $Y_{\rm D}$ tracks the equilibrium value $Y_{\rm D}^{\rm NSE}$ until the destruction rate $\lambda_\gamma Y_\gamma \approx 5\times 10^9 \exp(-Q/T_9)$ $\langle\sigma v\rangle_{pn{\rm D}\gamma}$ falls below the expansion rate. (The expression for the reverse rate follows from the formalism developed by Fowler, Caughlan, & Zimmerman 1967.) At this time, $Y_{\rm D}$ freezes out at approximately $Y_{\rm D}^{\rm FO} \approx Y_p Y_n T_9^3(\tau_{-5}/s_5)$. Here τ_{-5} is the dynamic timescale in units of 10^{-5} s and s_5 is the entropy per baryon in units of 10^5. This result implies that for $(\tau_{-5}/s_5) > 10^{-1}$, i.e., for essentially all reasonable fireball parameters, there is time to form interesting abundances of ^{2}H. In this case, the final ^{2}H abundance is limited by the flow to heavier nuclei.

To estimate the effects of flow to heavier nuclei, we employ the code developed by WFH67 and subsequently modified by Kawano. This code contains a reaction network for 26 light nuclei and rates for the relevant weak processes. The parameters of the "universe" relevant for BBN are the following: Hubble constant $H = \tau_{\rm dyn}^{-1}$, a freely chosen initial n/p (in contrast to BBN, where n/p is initially determined by weak reactions and assumed lepton numbers/spectra), and a final baryon-to-photon ratio $\eta \approx 3.6/(s/k_{\rm B})$. Note that the η relevant for these relativistic winds is some 5 orders of magnitude larger than the primordial value ($\eta \sim 6\times 10^{-10}$) and that the dynamic timescale for relativistic winds can be 7 orders of magnitude smaller than the dynamic timescale of $\sim$100 s characterizing the epoch of BBN.

In Figure 1 we show the evolution with time of the mass fractions of four light nuclei for winds with an entropy per baryon $s/k_{\rm B} = 10^5$ and differing dynamic timescales $\tau_{\rm dyn} = 10^{-3}$, 10^{-4}, 10^{-5}, and 10^{-6} s. This figure illustrates the effects of the competition between production and pho-

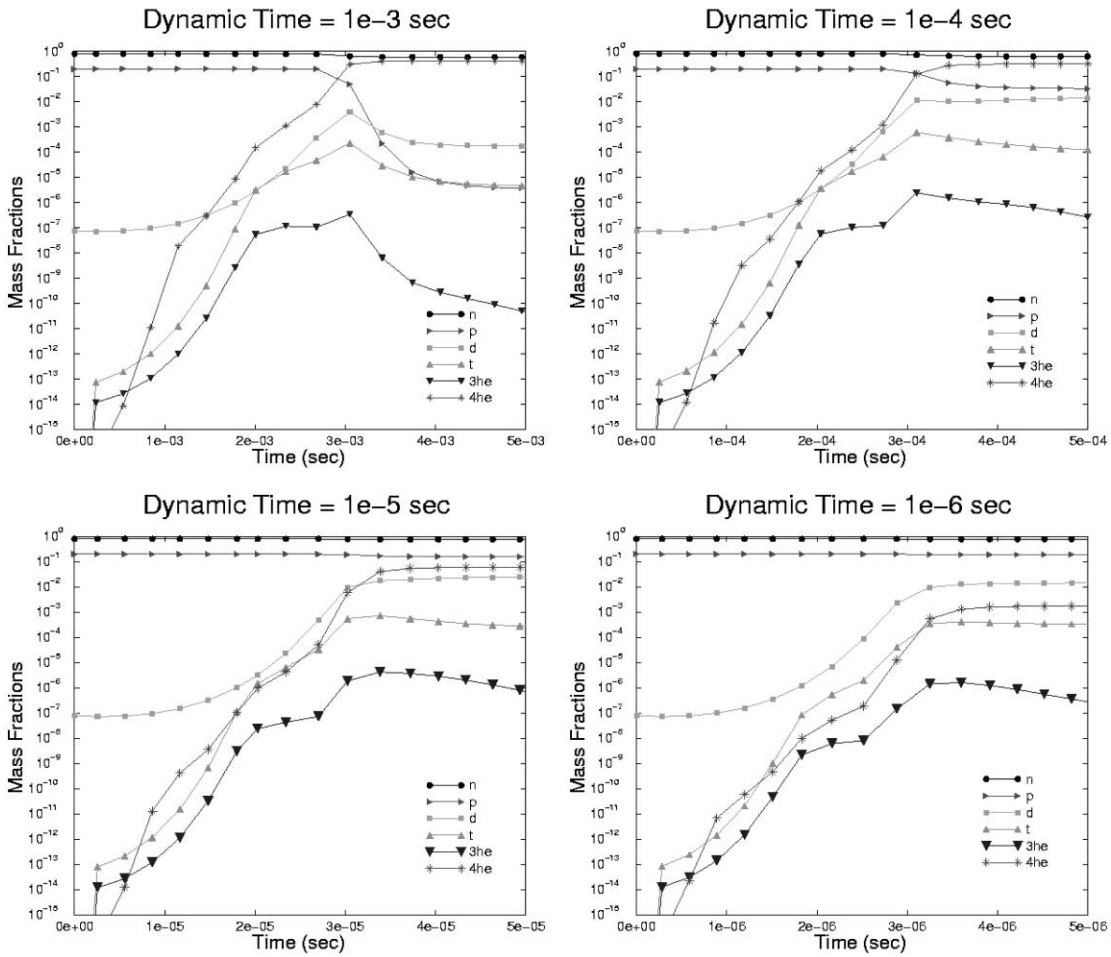

FIG. 1.—Evolution with time of the light-element mass fractions for four different wind cases. For each case, the entropy per baryon is 10^5, and Y_e is 0.2. The initial temperature in each calculation is 2 MeV.

todissociation of ^{2}H for outflows with a short dynamic timescale, and the flow to heavier nuclei for outflows with long dynamic timescales. For $\tau_{\rm dyn} = 10^{-6}$ s, the particle capture reactions out of deuterium are too slow to influence ^{2}H/H, and $Y_{\rm D}$ freezes out at approximately $Y_{\rm D}^{\rm FO} \approx 1/80$. For $\tau_{\rm dyn} = 10^{-5}$ s, flow to heavier nuclei, principally via $d(d,\ n)^3$He, $d(d,\ p)t$, and $t(d,\ n)^4$He (here t represents the triton, d represents the deuteron, and the three rates make roughly equal contributions), becomes important and depletes about 90% of the deuterium produced through $p(n,\ \gamma)d$. Of these depleted deuterons, approximately 0.1% are lost via $d(p,\ \gamma)^3$He [or $d(n,\ \gamma)t$ for neutron-rich material]. The evolution is similar for outflows with longer dynamic timescales, with flow to heavier nuclei becoming increasingly important with time. The reaction $d(p,\ \gamma)^3$He begins to dominate as the final $Y_{\rm D}$ decreases, and the ratio $Y_p\, Y_{\rm D}\sigma[d(p,\ \gamma)^3{\rm He}]/Y_{\rm D}\, Y_{\rm D}\sigma[d(d,\ n)^3{\rm He}] \approx 10^{-5}\, Y_p/Y_{\rm D}$ (at $T_9 = 1$) approaches unity. This is the case for the $\tau_{\rm dyn} = 10^{-3}$ s wind, and near this $\tau_{\rm dyn}$, the final $Y_{\rm D}$ is very sensitive to small changes in the entropy and dynamic timescale. This is also the regime most like BBN.

In Figure 2 we display the final ^{2}H abundance for the range of entropy and dynamic timescales of relevance to astrophysical sites. For this figure, we assume an initial electron fraction $Y_e = 0.5$. Note that for expansion timescales comparable to the free neutron lifetime, the final yields are sensitive to the temperature at which the neutron-to-proton ratio is specified. We show these very long expansion timescales only for illustrative purposes. The two top contours in Figure 2 correspond to deuterium production being limited by $d(\gamma,\ n)p$, and the two bottom contours correspond to deuterium production being limited by flow out of ^{2}H to heavier nuclei, principally by the strong interactions. Note, however, that at the lowest entropies in Figure 2, our estimates are approximate owing to the neglect of heavier species in the reaction network.

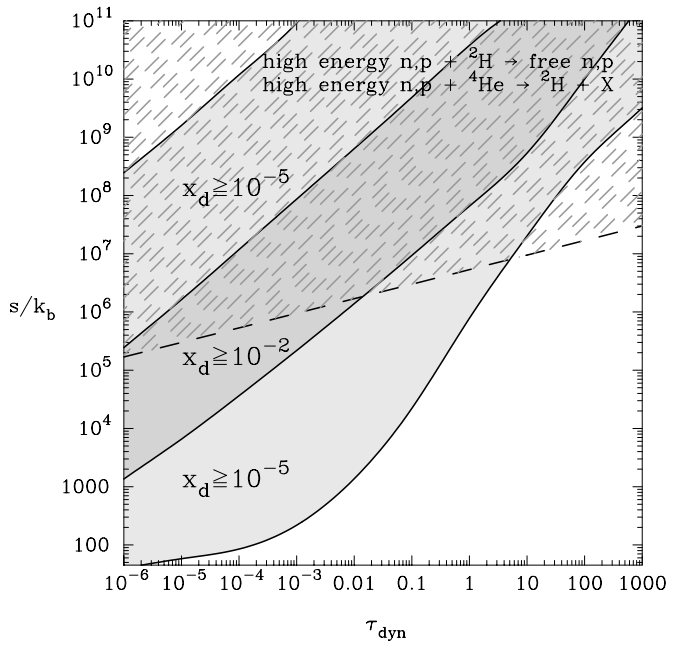

FIG. 2.—Final deuterium yield as a function of the dynamic timescale and entropy per baryon characterizing the relativistic flow for $Y_e = 0.5$. The initial temperature for each point was chosen as 0.5 MeV, and $\tau_{\rm dyn}$ is given in seconds. The shaded contours were calculated under the assumption that the neutrons remain well coupled kinematically to the flow. The top two lines correspond to ^{2}H production being limited by photodissociation, while the bottom two lines correspond to ^{2}H production being limited by the flow to ^{4}He. The thick dashed line is the neutron-decoupling line as described in the text. Above this line, the assumption of kinematically coupled neutrons breaks down, and high-energy nucleon-nucleus collisions change the nucleosynthesis.

The thick dashed line in the top half of the graph delimits the region in which dynamic neutron decoupling occurs. Dynamic neutron decoupling occurs because photons and $e^{\pm}$ pairs dominate the dynamics of the accelerating flow. Protons and charged nuclei are coupled to the relativistic light particles electromagnetically, but free neutrons are uncharged and have a small magnetic moment, so they are dragged along only by neutron-proton collisions. When these collisions become slower than the dynamic expansion timescale, the neutrons are left to coast, while the protons accelerate without them. In the absence of bound nuclei, the condition that dynamic neutron decoupling occurs is that $\tau_{\rm dyn} n_p \langle \sigma v \rangle_{\rm np} < 1$ before the end of the acceleration phase of the fireball's evolution (here n_p is the number density of protons). Putting in the scaling relations describing the evolution of the fireball gives this condition as $s/10^5 > 3(\tau_{\rm dyn}\, Y_p/10^{-5})^{1/4}$ (e.g., Fuller et al. 2000).

The precise neutron-decoupling condition depends on the nuclear composition of the flow. If, for example, all of the nuclei are locked into α-particles, then neutron decoupling cannot occur. Roughly, the fraction of nucleons bound in nuclei is small ($\lesssim 10\%$) for $\tau_{\rm dyn} < 10^{-4}$ s and entropies along the neutron-decoupling line, and the fraction of nucleons bound into α-particles approaches saturation for $\tau_{\rm dyn} > 10^{-4}$ and entropies along the neutron-decoupling line. This implies that for longer dynamic timescales, neutron decoupling will only occur if the flow is neutron rich or if the entropy is a factor of a few higher than that given by the neutron-decoupling line in the figure.

If the flow is neutron rich, neutron decoupling will result in high-energy (several hundred MeV) neutron-nucleus collisions, which will destroy and synthesize nuclei. These nonthermal reactions are not described by the Kawano reaction network. The net result of these collisions depends on the nuclear composition at the time of decoupling.

We consider two instructive limiting cases: (1) deuteron-rich and α-poor, and (2) deuteron-poor and α-rich. Case 1 occurs for short dynamic timescales and for entropies well above the neutron-decoupling line, while case 2 occurs for longer dynamic timescales and entropies near the neutron-decoupling line. The final nucleosynthesis is also sensitive to the (unknown) details of neutron decoupling. In particular, we see that the final deuterium abundance is sensitive to the exact number of high-energy interactions suffered by the average nucleus. This number is certainly between 1 and a few, but the exact number can only be obtained with a detailed transport calculation.

Any deuterons present when neutron decoupling occurs are destroyed. Likewise, any α-particles present are broken apart. Because the branching ratio for $\alpha+$ ($\sim$1 GeV nucleon) $\rightarrow {}^2{\rm H} + {\rm X}$ is high, about 50% (Dimopoulos et al. 1988), the production of ^{2}H through the spallation of α-particles may (over)compensate the loss of deuterium in direct collisions. Certainly for case 1, the α-poor case, neutron decoupling results in a net decrease in deuterium. For case 2, in which α-particles dominate, neutron decoupling drives $Y_{\rm D}$ to approximately one-half of the initial (i.e., at the beginning of neutron decoupling) value of

Y_α, provided that the average nucleus only undergoes one high-energy collision. If the average nucleus undergoes a few high-energy collisions, the nucleosynthesis is somewhere in between the one-collision case and the fixed-point case discussed by Dimopoulos et al. (1988).

For example, if initially the material is composed entirely of α-particles and free neutrons, and each α-particle suffers one high-energy collision with a neutron, then $\sim$10% of the material will be converted to ^{2}H. Regions in Figure 2 above the decoupling line in which the freezeout mass fraction of α-particles is large could approximate this case. If in addition this initial spallation takes place right at the neutron-decoupling point, then none of the deuterium produced from the fragmenting of α-particles will be destroyed. Only if these conditions are met can the final ^{2}H yield be as high as $\sim$10%.

Note that here there is no source of significant postnucleosynthesis photodissociation of deuterium. This is because on average there is only $\sim$100 MeV per baryon in the form of electromagnetic radiation coming from the decay of pions produced in inelastic nucleon-nucleon collisions. This is 3 orders of magnitude smaller than the $\sim$100 GeV per baryon coming from the decay of massive particles discussed by Dimopoulos et al (1988). In addition, here the energy injection by π- and μ-decay is well approximated as occurring at the decoupling temperature $T_{\rm D} \approx 0.005(s_5/\tau_{-5}\,Y_e)^{1/3}$ MeV . This means that, unlike the case in which a massive particle decays with a lifetime of many system dynamic timescales, the maximum energy of the nonthermal breakout photons does not keep rising with time. Interestingly, the recognition that the branching ratio for ^{2}H production in high-energy nucleon–α-particle collisions is so large suggests that relativistic flows might lead to direct deuterium production via collisions with dense winds or ejecta surrounding the site of the relativistic wind (G. M. Fuller, S. Guiles, & J. Pruet 2002, in preparation).

In Figure 3 we illustrate the effect that changing the neutron-to-proton ratio has on the nucleosynthesis. Two illustrative examples are shown. The top curve corresponds to a high-entropy, short–dynamic timescale expansion, and there is little synthesis of nuclei heavier than ^{2}H. In this case, the final deuterium abundance follows a clean, simple freezeout from NSE, i.e., the Saha equation: $Y_{\rm D} \propto Y_p\,Y_n \approx Y_e(1 - Y_e)$, where Y_e is the number of electrons per baryon. The bottom line in Figure 3 corresponds to a lower entropy and can be thought of as a convolution of the top curve with the reactions $d(d,\ n)^3$He and $d(d,\ p)t$. The effect of destruction is less pronounced on the wings of the curve simply because the deuterium abundance is smaller and the reactions $d(d,\ n)^3$He (and other comparable reactions) are slower.

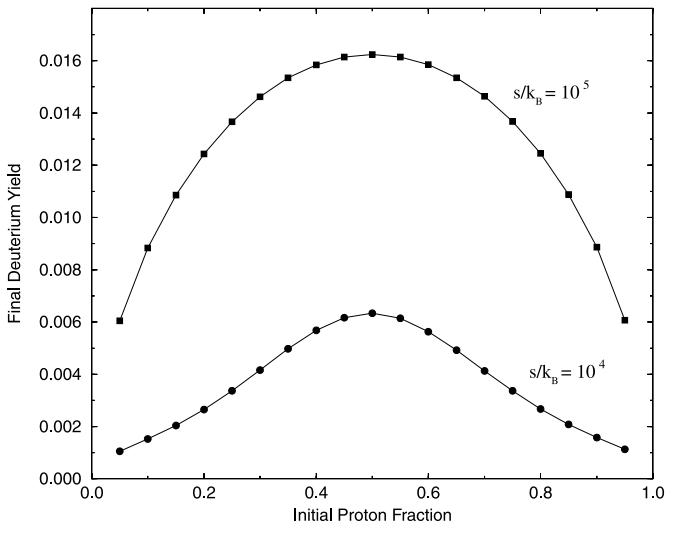

FIG. 3.—Final deuterium yield as a function of the electron fraction. The top curve is for $\tau_{\rm dyn} = 10^{-5}$ s and $s/k_{\rm B} = 10^5$, while the bottom curve is for $\tau_{\rm dyn} = 10^{-5}$ s and $s/k_{\rm B} = 10^4$. The initial temperature here was chosen as 0.3 MeV.

At this point, we can address in a broad stroke the issue of deuterium production in proposed GRB models. For long bursts, observed redshifts imply a total energy output in GRBs of the order of 10^{53}–$10^{54}(\Omega/4\pi)$ ergs. Here Ω is the opening angle subtended by the relativistic outflow. There is some evidence that long GRBs are typically beamed by a factor of $\Omega/4\pi \approx 1/500$ and that the total energy output in long GRBs is roughly burst independent and about 10^{51} ergs. For short GRBs, no redshifts have been measured, and little is known about the energy scale. Not all of the energy E_0 can be converted to gamma rays, and E_0 is larger than the energy in gamma rays by at least a factor of 5–10. An estimate of the energy scale gives the initial temperature in GRBs:

$$T_0 \approx 10\ {\rm MeV}\left[\frac{E_0}{10^{52}\ {\rm ergs}}\left(\frac{4\pi/\Omega}{500}\right)\frac{10\ {\rm s}}{T_{\rm burst}}\left(\frac{10^6\ {\rm cm}}{R_0}\right)^2\right]^{1/4}. \quad (4)$$

The Lorentz factors invoked to explain GRBs lie in the range $\sim 10^2$–10^3, with the smaller values corresponding to internal-shock models for long bursts and the larger values corresponding to external-shock models for short bursts. This implies entropies per baryon in the range of 10^4–10^6. From Figure 2 we see that very compact central engines, characterized by short dynamic timescales and high entropies, are typically associated with substantial thermal or nonthermal deuterium production. Examples of such central engines are the merger model of Mészáros & Rees (1997) and the supranova model of Vietri & Stella (1998). On the other hand, the long dynamic timescales and smaller entropies characteristic of, e.g., the collapsar model (Woosley 1993) are more α-rich and deuteron poor.

3. CONCLUSION AND DISCUSSION

There are three length scales discussed in connection with GRBs. The first is the size of the central engine ($R_0 \sim 10^6$ cm for compact objects; $R_0 \sim 10^{11}$ cm for collapsars). This region has been the focus of many detailed attempts at understanding the dynamics of the collapsing object giving rise to the relativistic flow. The second length scale is the scale associated with the shocking that generates the observed signal: $\gamma_f^2 R_0$ for internal shocks or $\sim 10^{15}$ cm for external shocks. For obvious reasons, this scale has also been the subject of many studies. In this paper we have considered a third, intermediate scale ($\sim\gamma R_0$) associated with the acceleration of the thermal fireball. This region is rich in nuclear and particle phenomena and is the only region sensitive to, e.g., the neutron-to-proton ratio in the flow.

We have explored nucleosynthesis for the broad range of dynamic timescales, neutron-to-proton ratios, and entropy per baryon that can be found in these relativistic flows surrounding stellar endpoint events. For relativistic flows for which the neutrons remain kinematically well coupled, the nucleosynthesis is similar to the freezeout nucleosynthesis discussed in connection with BBN. The final mass fraction of deuterium can be greater than a few percent, some 3 orders of magnitude larger than the primordial value. For flows for which the assumption of kinematically well-coupled neutrons breaks down, we find that light-element synthesis is dominated by high-energy nonthermal nucleon-nucleus collisions. In these latter cases, the deuterium number fraction can be high, $Y_{\rm D} \lesssim 10\%$. This local overabundance of deuterium resides in the shell propagating into the ISM at late times. Recently, these shells have gained some attention because a radio identification of a young ($\sim$ 100 yr) nonspherical H I shell might tell us something about GRBs and their association with supernovae (Paczyński 2001).

Whether or not the deuterium produced in stellar endpoint events is detectable depends ultimately on the degree of mixing with the ISM. The total amount of mass in deuterium produced in these events is $M_{\rm D} \approx 10^{-6}\ M_{\odot}(E/10^{52}\ {\rm ergs})(100/\gamma_f)(Y_{\rm D}/10^{-2})$, where E is the total energy in the relativistic flow. For H I column densities of the order of $10^{19}\ {\rm cm}^{-2}$, this deuterium leads to a factor of 2 increase in $^2{\rm H}/{\rm H}$ over the primordial $^2{\rm H}/{\rm H}$, as long as it mixes in a volume less than about a cubic light year. Structures of this size associated with nearby supernova remnants are seen and resolved with the Very Large Array. However, even with the most optimistic assumption that every supernova is accompanied by a relativistic wind, the mechanism discussed here can only contribute to the *overall* present-day deuterium abundance at the level of about 0.1%.

It is perhaps frustrating then that such a prodigious yield of deuterium has little leverage on the scale of the cosmological abundance. However, the potentially large ^{2}H production in relativistic flows could possibly be detectable and therefore provide a new probe of, e.g., GRB central engine physics and expansion dynamics.

We acknowledge discussions with K. Abazajian, D. Kirkman, J. O'Meara, and S. Woosley. This work was supported in part by NSF grant PHY 00-99499 at the University of California, San Diego (UCSD), and Department of Energy Sci-Dac supernova grants at Lawrence Livermore National Laboratory and UCSD.

A preprint by Lemoine (2002) appeared almost concurrently with ours and discusses many of the same issues we do. Lemoine discusses in some detail the influence of nonthermal energy sources in the fireball on nucleosynthesis and also points out that nucleosynthesis in relativistic flows may lead to a weakening of the neutrino signal expected from the decay of pions created in inelastic nucleon-nucleon collisions occurring during neutron decoupling.

REFERENCES

Dimopoulos, S., Rahim, E., Hall, L., & Starkman, G. 1988, ApJ, 330, 545
Eichler, D., Livio, M., Piran, T., & Schramm, D. N. 1989, Nature, 340, 126
Fowler, W. A., Caughlan, G. R., & Zimmerman, B. A. 1967, ARA&A, 5, 525
Fuller, G. M., Pruet, J., & Abazajian, K. 2000, Phys. Rev. Lett., 85, 2673
Kawano, L. 1992, Let's Go Early Universe, FERMILAB-Pub-92/04-A, Fermilab
Lemoine, M. 2002, A&A, submitted (astro-ph/0205093)
MacFadyen, A. I., & Woosley, S. E. 1999, ApJ, 524, 262
McCullough, P. R. 1992, ApJ, 390, 213
Mészáros, P., Laguna, P., & Rees, M. J. 1993, ApJ, 415, 181
Mészáros, P., & Rees, M. J. 1997, ApJ, 482, L29
Meyer, B. S., Mathews, G. J., Howard, W. M., Woosley, S. E., & Hoffman, R. D. 1992, ApJ, 399, 656
O'Meara, J., Tytler, D., Kirkman, D., Suzuki, N., Prochaska, J., Lubin, S., & Wolfe, A. 2001, ApJ, 552, 718
Otsuki, K., Tagoshi, H., Kajino, T., & Wanajo, S. 2000, ApJ, 533, 424
Paczyński, B. 1990, ApJ, 363, 218
———. 2001, Acta Astron., 51, 1
Piran, T. 1999, Phys. Rep., 314, 575
Pruet, J., Fuller, G. M., & Cardall, C. Y. 2001, ApJ, 561, 957
Takahashi, K., Witti, J., & Janka, H. T. 1994, A&A, 286, 857
Thompson, T., Burrows, A., & Meyer, B. 2001, ApJ, 562, 887
Vietri, M., & Stella, L. 1998, ApJ, 507, L45
Vlahakis, N., & Königl, A. 2001, ApJ, 563, L129
Wagoner, R. V., Fowler, W. A., & Hoyle, F. 1967, ApJ, 148, 3 (WFH67)
Woosley, S. E. 1993, ApJ, 405, 273
Woosley, S. E., Wilson, J. R., Mathews, G. J., Hoffman, R. D., & Meyer, B. S. 1994, ApJ, 433, 229